RESEARCH ARTICLE

Exploring seasonal variability in water quality of Nyabarongo River in Rwanda via water quality indices and DPSIR modelling

Mycline Umuhoza[1] · Dongjie Niu[1,2,3] · Fengting Li[1,2,3]

Abstract

Understanding seasonal variations in water quality is crucial for effective management of freshwater rivers amidst changing environmental conditions. This study employed water quality index (WQI), metal index (MI), and pollution indices (PI) to comprehensively assess water quality and pollution levels in Nyabarongo River of Rwanda. A dynamic driver-pressure-state-impact-response model was used to identify factors influencing quality management. Over 4 years (2018–2021), 69 samples were collected on a monthly basis from each of the six monitoring stations across the Nyabarongo River throughout the four different seasons. Maximum WQI values were observed during dry long (52.90), dry short (21.478), long rain (93.66), and short rain (37.4) seasons, classified according to CCME 2001 guidelines. Ion concentrations exceeded WHO standards, with dominant ions being HCO_3^- and Mg^{2+}. Variations in water quality were influenced by factors such as calcium bicarbonate dominance in dry seasons and sodium sulfate dominance in rainy seasons. Evaporation and precipitation processes primarily influenced ionic composition. Metal indices (MI) exhibited wide ranges: long dry (0.2–433.0), short dry (0.1–174.3), long rain (0.1–223.7), and short rain (0.3–252.5). The hazard index values for Cu^{2+}, Mn^{4+}, Zn^{2+}, and Cr^{3+} were below 1, ranging from $8.89E-08$ to $7.68E-07$ for adults and $2.30E-07$ to $5.02E-06$ for children through oral ingestion, and from $6.68E-10$ to $5.07E-07$ for adults and $6.61E-09$ to $2.54E-06$ for children through dermal contact. With a total carcinogenic risk of less than 1 for both ingestion and dermal contact, indicating no significant health risks yet send strong signals to Governmental management of the Nyabarongo River. Overall water quality was classified as marginal in long dry, poor in short dry, good in long rain, and poor again in short rain seasons.

Graphical Abstract
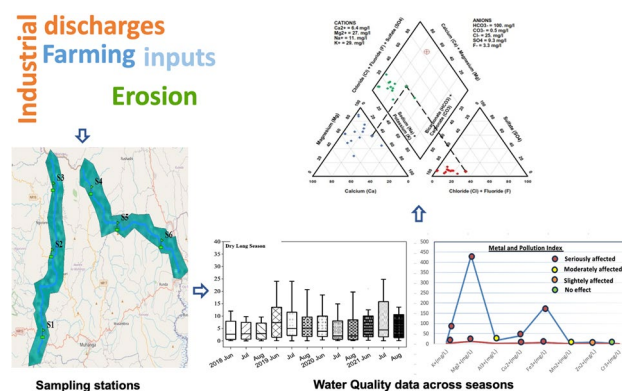
Responsible Editor: Xianliang Yi

Extended author information available on the last page of the article

Introduction

Ensuring access to clean water is vital for preserving ecosystem health and upholding the functionality of global production systems (Halisçelik and Soytas 2019). Throughout history, rivers have served as foundational elements in the advancement of civilizations, with human settlements heavily reliant on these freshwater reservoirs. However, in the wake of industrialization and intensified agricultural activities, the quality of water in perennial rivers worldwide is witnessing a steady decline (Kumar et al. 2018). This trend is particularly pronounced in Africa, where water pollution has been exacerbated across nearly all river systems since the 1990s, exposing hundreds of millions of people to health risks due to contaminated surface waters (Chen and Shen 2022). Hence, monitoring river water quality serves as an initial stride in formulating strategies for managing freshwater reservoirs to mitigate the risks of waterborne disease.

Monitoring the spatial and temporal dynamics of a set of parameters is a common approach for assessing the surface water quality of a river catchment. Water quality data can include measurements made in the field, water samples collected and analyzed in the laboratory, or information extracted from other data sets or geographic information layers (Basin 2022). This comprehensive approach allows a better understanding of the overall water quality and its impact on ecosystems, human health, and activities. Many countries regularly evaluate water quality in rivers as part of national water monitoring systems (European Environment Agency 2020). These evaluations are conducted through field inventories, which involve the collection and analysis of water samples to assess various parameters that indicate the health and safety of water bodies. For instance, the Environmental Protection Agency (EPA) in the USA conducts the National Water Quality Inventory, which summarizes the findings of both national surveys and site-specific assessments (European Environment Agency 2017). Water quality monitoring efforts by organizations such as the Interstate Commission on the Potomac River Basin (ICPRB) and the US National Park Service (NPS) focus on measuring, analyzing, planning, acting, and educating to ensure the health of rivers and their surrounding ecosystems (European Environment Agency 2020). These efforts include collecting water quality and habitat data, assisting in the establishment of water quality criteria, and developing total maximum daily loads (TMDLs) (Basin 2022).

In many tropical countries, the lack of specific organizations for monitoring water quality in rivers, as well as financial and human resource constraints, can limit the coverage and frequency of field inventories (Kayembe et al. 2018, Camara et al. 2019). The Nyabarongo River, as an essential freshwater source in Rwanda, is facing significant challenges in terms of water quality (Kulimushi et al. 2021). The river is heavily relied upon by the people for various domestic and industrial needs, yet for decades its contamination has been one of Rwanda's most critical water-related issues (Nteziyaremye and Omara 2020, Nteziyaremye et al. 2020). There is an existing paucity of data on the water quality of the Nyabarongo River, making it difficult to determine an appropriate site-specific index for policy and management of the river. Previous studies have shed some light on the ecological status of the river; for example, the bioaccumulation of heavy metals in the West African lungfish (*Protopterus annectens*) has been examined, and the concentrations were found to be above the threshold limits (Nteziyaremye and Omara 2020, Nteziyaremye et al. 2020). Soils within the Nyabarongo catchment areas were also found to contain high levels of persistent organic pollutants, which can erode into the river during heavy rainfall (Umulisa et al. 2020). To the author's best knowledge, there is no specific research output quantifying the water quality status of the Nyabarongo River to determine an appropriate site-specific index that could serve as a basis for river policy and management.

Several conceptual frameworks have emerged to examine the impact of human activities on the environment. These include the pressure-state-response (PSR) framework (Li et al. 2021), the driver-pressure-state-impact-response (DPSIR) framework (Qin et al. 2003), the IPAT equation (impact = population × affluence × technology) (Yan Zhou 2016), and the socio-ecological systems framework (Chen et al. 2024). Among these, the DPSIR model stands out for its comprehensive approach to understanding the complex relationship between human actions and the environment, making it particularly valuable for studying seasonal variations in water quality (He et al. 2022). Understanding these seasonal fluctuations in water quality is crucial for assessing their Impacts on human health, aquatic ecosystems, and socioeconomic activities reliant on the river. Applying the DPSIR model allows for the identification of primary factors contributing to water quality decline, evaluating their seasonal impacts, and crafting specific responses like enhancing agricultural methods, implementing watershed management plans, and enacting pollution control measures (Wang et al. 2022b).

The main objective of this study was to analyze and depict the fluctuations in water quality attributes across both space and time in the Nyabarongo River situated in Rwanda. Moreover, the study sought to perform a thorough evaluation of water quality utilizing the water quality index (WQI) methodology. Additionally, it endeavored to estimate the potential health hazards stemming from heavy metal

contamination in the river. Furthermore, the research aimed to pinpoint and comprehend the primary factors influencing water quality, along with the pressures and impacts on its condition. To accomplish these goals, a DPSIR model was developed to bolster the management system of the river; three indices were utilized, specifically the drinking water quality index (DWQI), metal index (MI), and pollution index (PI) to assess the water quality of the Nyabarongo. Twenty-three water quality parameters were selected, and measurements were conducted monthly at six water quality monitoring stations within the study area. This data collection spanned from January 2018 to December 2021, ensuring a robust dataset for developing a water quality index (WQI) specifically for the Nyabarongo River of Rwanda. The outcomes of this investigation are poised to enhance the understanding of the current water quality status in the Nyabarongo River and facilitate the sustainable management of surface water resources in Rwanda.

Materials and methods

Study area

The Nyabarongo River plays a critical role as a primary freshwater source in Rwanda, serving as a crucial dependency for the populace's various domestic and industrial requirements (Kulimushi et al. 2021). The Nyabarongo River starts from the confluence of the Mbirurume and Mwogo Rivers and ends up at its confluence with the Akanyaru River, emptying into the Akagera River, one of the largest rivers that drain into Lake Victoria (Benjamin 2015). The major tributaries are the Akanyaru River from the South and the Mukungwa River from the north, emerging from the volcanoes. The river catchment area covers 17 districts from all the provinces of the country and the City of Kigali.

Nyabarongo River (Fig. 1) is part of the upper headwaters of the Nile River with an approximate length of 151.5 km and drains a total area of 8478.24 km^2 in its catchment zone (Umulisa et al. 2020). The catchment is formed by mountainous terrains with a mean slope of approximately 30% and elevation ranging from 1341 to 4491 m. The geological formation consists of 59% Acrisols, 19.2% Regosols, 9.2% Andolsols, 6.7% Ferralsols, 2.8% Cambisols, 0.8% Histosols, and 0.4% Gleysols (Holzforster and Schmidt 2007). The catchment experiences a tropical climate with two rainfall seasons a year, March to May and September to December. The temperature within the catchment can reach a maximum daily of 25.3 °C and a minimum of 14.6 °C in the western part and 23.6 °C and a minimum daily temperature of 14.0 °C in the southern part (Kwisanga 2017). Precipitation increases with elevation, which varies from about 864 mm in the central plateau
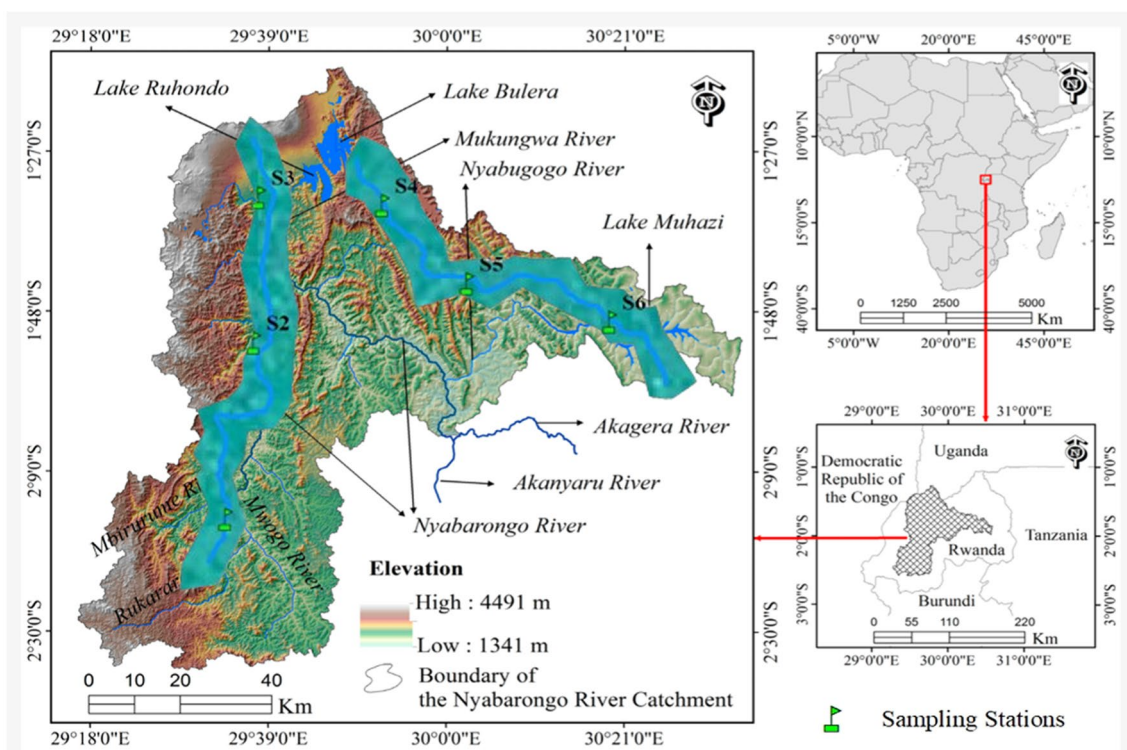
Fig. 1 The study location and sampling stations along the Nyabarongo river

across Lake Muhazi and Kigali City to 2258 mm in the mountain ranges over Nyungwe forest and volcano areas (Karamage et al. 2016).

Methodologies

Based on the objectives of this study, a dynamic DPSIR model was utilized to identify factors affecting quality management. Furthermore, the researchers collected water quality data from the period of 2018 to 2021 obtained from six sampling stations to be analyzed. Sixty-nine samples were collected monthly from each station. The stations were chosen strategically in consideration of the pressures on the Nyabarongo.

The sampling regimes and data gathering were concurrent with periodic monitoring activities of the Waste and Sanitation Company (WASAC) of Rwanda to compare results. Additional water quality data for the period of 2018–2020 was provided by WASAC. Water samples were collected throughout the years to coincide with the four major climate seasons of Rwanda in Table 1. Before each sampling event, 25 mL sample bottles were rinsed with dilute ethanol and air-dried overnight at room temperature (± 23 °C). All in situ monitoring instruments were calibrated, and at the site, sample bottles were rinsed with water three times before sampling. The samples were collected to minimize water bubbles collecting in the bottles.

Standard methods prescribed by the American Public Health Association (American Public Health Association 1999) were employed for the analysis of water samples. Water pH and temperature are determined in situ using a Hanna HI9812 combo meter, and in the laboratory, pH of stored water is determined by potentiometry before every analysis. Major cations are analyzed by atomic absorption spectrophotometry (AAS).

- AAS analytical procedure

1. Sample preparation

Table 1 Climate seasonal pattern of Rwanda

Season	Period	Description
Dry short	December–February	Dry periods with occasional rainfall
Long rain	March–May	Major wet period with high rainfall
Long dry	June–August	Major dry periods with least rainfall
Short rain	September–November	Wet periods with occasional rainfall

Water samples underwent collection following appropriate protocols to prevent contamination. Depending on the targeted cations, some samples were either filtered or subjected to acidification to eliminate interfering substances.

2. Calibration

Calibration standards were established by diluting stock standard solutions of the relevant cations to concentrations spanning the expected range in the samples.

3. Instrument configuration

The AAS instrument underwent calibration using standard solutions specific to each cation. Parameters such as wavelength, lamp current, and slit width were adjusted accordingly.

4. Sample analysis

Samples were introduced into the flame, and the absorbance of each cation's characteristic wavelength was measured. Utilizing the calibration curve aided in determining the concentration of each cation in the sample.

5. Quality control

Regular checks were conducted on instrument performance using control standards. Additionally, accuracy and precision were verified through replicate analyses and spike tests.

- Utilized equipment

1. Atomic absorption spectrophotometer

This equipment comprises a light source (hollow cathode lamp or electrodeless discharge lamp), a monochromator, a sample introduction system (flame or graphite furnace), and a detector.

2. Graphite furnace atomizer

Primarily employed for trace analysis due to its heightened sensitivity and reduced interference compared to flame atomization.

3. Sample introduction system

Flame AAS consists of a nebulizer, spray chamber, and burner head. In the case of graphite furnace AAS, it involves a graphite tube and heating system.

4. Calibration standards and reagents

Included stock standard solutions for each targeted cation, dilution solutions, and matrix modifiers for complex samples.

• Analytical standards

1. Accuracy

Ensured through the analysis of certified reference materials (CRMs) possessing known concentrations of the cations.

Precision

Evaluated by conducting replicate analyses of identical samples or by employing control charts.

2. Detection limits

Determined based on signal-to-noise ratios or standard deviation methods for each cation.

Interference

Minimized by utilizing suitable matrix modifiers or selecting wavelengths with minimal interference.

3. Quality assurance

Adherence to standardized protocols for quality assurance and quality control (QA/QC) to guarantee result reliability.

Quality assurance and quality control (QA/QC) procedures of analytical and instrument methods were confirmed in the WASAC laboratory which includes 5% repeats, standard calibration curves, and quality control reference standards. Standard curves are generated for every analysis regime. The method detection limits (MDLs) of the reference standard were applied. Table 2 shows general water

quality assessment criteria as recommended by the Canadian Council of Ministers Environment (CCME), while Table 4 shows various parameters involved in the WQI assessment.

In addition to the standard analytical procedures described, we calculated the charge balance error (CBE) for each water sample to assess the accuracy of our ionic concentration measurements. The CBE ranged from -4 to $+5\%$, which is within the $\pm 5\%$ range considered acceptable for hydro chemical analyses. All statistical tests in this study were performed with a significance level set at 0.05, corresponding to a 95% confidence level.

In this study, we conducted T-tests to analyze the temporal variation in water quality parameters over a 4-year period. The results revealed a T-test value of 0.85, indicating significant differences in water quality among the years assessed.

This suggests notable shifts in water quality over the study period. Such findings underscore the necessity for ongoing monitoring efforts and targeted interventions to mitigate environmental risks and safeguard water resources.

Indexing approach

Different approaches, which were governed by three factors including parameter selection, quality function calculation (sub-index), and accumulation of sub-indices, were applied using arithmetic equations and compared to evaluate the suitability of collected water samples along the Nyabarongo River (Mohseni et al. 2022). The suitability of surface water for drinking and its sensitivity to pollution were investigated using WQI, MI, and PI, which were calculated using physical and chemical properties.

For potable water quality assessment, the findings on 23 physicochemical parameters of collected samples were considered. The physical and chemical parameters were weighted based on their significance to the total quality of water. The WQI reflects the total water quality of water variables based on a combination of water characteristics and their utilization in the ecosystem (Brown et al. 1972) as indicated in Eq. (1);

Table 2 Water quality index criteria

Category	WQI value	Description
Excellent	95–100	Water quality is protected with a virtual absence of threat or impairment; conditions very natural or pristine levels
Good	80–94	Water quality is protected with only a minor degree of threat or impairment, coordinates rarely depart from natural or desirable levels
Fair	65–79	Water quality is usually protected but occasionally threatened or impaired, conditions sometimes depart from natural or desirable levels
Marginal	45–64	Water quality is frequently threatened, or impaired conditions often depart from natural or desirable levels
Poor	0–44	Water quality is almost always threatened or impaired; conditions usually depart from natural or desirable levels

Source: CCME (2001)

$$WQI = \sum_{i=1}^{n} Q_i W_i \tag{1}$$

According to the WHO (WHO 2017), the estimated value of $Q_i W_i$ is influenced by the concentration of each water component (C_i) and their guideline (S_i) for drinking water, as indicated in the following equations:

$$Q_i = \frac{C_i}{S_i} \times 100 \tag{2}$$

$$W_i = \frac{W_i}{\sum w_i} \times 100 \tag{3}$$

where W_i is the relative weight and w_i is the weight unit of each water component. Equation (4) is applied to determine the w_i for each component in accordance with the specified criteria for drinking water

$$w_i = K/S_i \tag{4}$$

K is the constant of proportionality, which can be computed using the following equation:

$$K = \frac{1}{\sum S_i} \tag{5}$$

To calculate the WQI, a weight for each surface water parameter (w) was assigned for pH, turbidity, TDS, EC, K^+, Na^+, Mg^{2+}, Ca^{2+}, Cl^-, SO_4^{2-}, HCO_3^-, CO_3^{2-}, Al^{3+}, Br^-, Cr^{3+}, Cu^{2+}, Fe^{3+}, Mn^{4+} and Zn^{2+}, CN^-, F^-, NO_3^-, and PO_4^{3-} and the quality rating range (Q) and relative weight (W_i) were estimated. The computed values of the standards, unit weights (w_i), and relative weights (W_i) for the surface water parameters are shown in Table 3. The derived WQI was compared to the CCME (Saffran et al. 2001)WQI index.

The pollution indices, such as metal index (MI) and pollution index (PI), were calculated for the concentrations of metals including Al^{3+}, Cr^{3+}, Cu^{2+}, Fe^{3+}, Mn^{4+}, Mg^{2+}, K^+, and Zn^{2+} using Eqs. (6) and (7).

Metal index (MI)

According to Eq. (6), the metal index (MI) was used to analyze the probable impact of metals on public health, which helps in swiftly estimating the overall quality of water (Tamasi and Cini 2004).

$$MI = \sum_{i=1}^{n} \frac{H_c}{H_{max}} \tag{6}$$

where H_c is the concentration of each metal in the collected water sample, H_{max} is the maximum limit concentration for

Table 3 WHO (2022) standards vs calculations of WQI based on arithmetic weight approach for physicochemical properties

ID	Parameters	WHO (2022) S_i	Unit weight w_i	Relative weight W_i
1	pH	8.5	0.000034	0.004450
2	Turb (NTU)	5	0.000057	0.007565
3	EC (μS/cm^3)	1500	0.000000	0.000025
4	TDS (mg/L)	500	0.000001	0.000076
5	HCO_3^- (mg/L)	120	0.000002	0.000315
6	CO_3^- (mg/L)	350	0.000001	0.000108
7	NO_3^- (mg/L)	50	0.000006	0.000756
8	PO_4^{3-} (mg/L)	50	0.000006	0.000756
9	SO_4^{2-} (mg/L)	250	0.000001	0.000151
10	Cl^- (mg/L)	75	0.000004	0.000504
11	Ca^{2+} (mg/L)	12	0.000024	0.003152
12	K^+ (mg/L)	200	0.000001	0.000189
13	Na^+ (mg/L)	250	0.000001	0.000151
14	Mg^{2+} (mg/L)	50	0.000006	0.000756
15	Al^{3+} (mg/L)	0.1	0.002871	0.378246
16	Cu^{2+} (mg/L)	2	0.000144	0.018912
17	Fe^{3+} (mg/L)	0.3	0.000957	0.126082
18	Mn^{2+} (mg/L)	0.1	0.002871	0.378246
19	Zn^{2+}(mg/L)	3	0.000096	0.012608
20	Br^-(mg/L)	2	0.000144	0.018912
21	CN^- (mg/L)	1	0.000287	0.037825
22	F^- (mg/L)	4	0.000072	0.009456
23	Cr^{3+} (mg/L)	50	0.000006	0.000756

each metal, and the subscript i is the ith sample (Ojekunle et al. 2016).

Pollution index (PI)

The PI values were used to evaluate the influence of metal pollution on surface water (Caeiro et al. 2005). According to Eq. 7, the PI is categorized into five groups as shown in Table 4, which reflects the distinct pollution influence from each metal on water quality.

$$PI = \frac{\sqrt{\left(\frac{C_i}{S_i}\right)^2_{max} + \left(\frac{C_i}{S_i}\right)^2_{min}}}{2} \tag{7}$$

where C_i represents the content of each metal in the collected sample and S_i represents the standard limit of each metal in potable water (Caeiro et al. 2005, Goher et al. 2019).

Table 4 Levels of pollution according to PI values

Class	PI Value	Effect
1	< 1	No Effect
2	1-2	Slightly affected
3	2-3	Moderately affected
4	3-5	Strongly affected
5	>5	Seriously affected

Health risk analysis

Assessing the risk of trace elements in water typically considers direct human intake and skin intake. The toxic effects of exposure to pollutants in adults and children were calculated according to the hazard index (HI) and carcinogenic risks (CR) approach offered by the USEPA.

Oral dose (M_{ing-s}):

$$M_{ing-s} = \frac{C_w \times IngR \times EF \times ED \times CF}{BW \times AT} \qquad (8)$$

Dermal dose (M_{der-s}):

$$M_{der} = \frac{C_w \times SA \times SL \times ABS \times EF \times ED \times CF}{BW \times AT} \qquad (9)$$

$$HI = \sum HQ_i = \sum \frac{ADI_{ij}}{RfD_{ij}}$$

$$TCR = \sum CR_i = \sum ADI_{ij} x SF_{ij}$$

where C_s is the concentration of pollutants in water (mg kg^{-1}), EF is the exposure frequency (days year^{-1}), ED is the exposure duration (years), IngR is the receptor water ingestion rate (mg day^{-1}), SA is the skin surface area available for exposure (cm^2), SL is the water-to-skin adherence factor (mg cm^{-2} event^{-1}), ABS is the dermal dimensionless factor, BW is the time-averaged body weight (kg), and AT is the average time of noncarcinogenic and carcinogenic risks (days). Specific parameters for the estimation of non-carcinogenic risk are provided in Table 5.

For non-carcinogenic risk (NCR), *HI* refers to all sum of *HQ* (hazard quotients) in heavy metals. *HI* > 1 represents the potential adverse effect on human health. For total carcinogenic risk (TCR) and carcinogenic risk (CR), the values

Table 5 Distributions of parameters for the health risk assessment of heavy metals

Parameter	Description	Units	Adult	Children
IRs	Ingestion rate of water	µg/L	100	200
EF	Exposure frequency	d·a^{-1}	350	320
ED	Exposure duration	years	24	6
BW	Average body weight	kg	56.8	15.9
AT-NC	Average exposure time	d	8760	2190
AT-C	Average exposure time	d	26,280	26,280
SA	Surface area of skin	(cm^2·d)$^{-1}$	2145	1150
AF/SL	Skin adherence factor	(cm^2·d)$^{-2}$	0.07	0.2
ABS-NC	Dermal absorption factor	-	0.001	0.001
ABS-C	Dermal absorption factor	-	0.001	0.001
PEF	Emission factor	m^3·kg^{-1}	1.36E+09	1.36E+09
CF	Conversion factor		1.00E−06	1.00E−06

NC-Non-carcinogenic; C-Carcinogenic

TCR and CR < 10^{-6}, 10^{-6} < TCR and CR < 10^{-4}, and TCR and 10^{-4} represent no health risk, no significant health risk, and high health risk, respectively (Zhang et al. 2020). The specific toxicity threshold (*RfD*, mg kg^{-1} day^{-1}) and slope factors (*SF*, mg kg^{-1} day^{-1}) values are presented in Table 6.

Data analysis

To ensure the appropriateness of statistical methods applied in this study, we conducted Shapiro–Wilk tests to assess the normality of the distribution of data collected from various monitoring stations along the Nyabarongo River. These

Table 6 Reference dose (RfD) and dermal permeability coefficient in samples (Kp), gastrointestinal absorption factor (ABSg), and slope factor (SF) of heavy metals used for health risk assessment

	$RfD_{ingestion}$ (µg/kg/day)	RfD_{dermal} (µg/kg/day)	Kp (cm/h)	$ABSg$	SF_{ing} (mg/kg/day)$^{-1}$	SF_{der} (mg/kg/day)$^{-1}$
Mn^{2+}	24	0.96	1×10^{-3}	6%		
Zn^{2+}	300	60	6×10^{-4}	20%		
Cr^{3+}	3	0.075	1×10^{-3}	3.5%	0.5	20
Cu^{2+}	40	8	1×10^{-3}	5.7%		

tests confirmed that the data were normally distributed, which justifies our use of parametric statistical methods for further analyses. Specifically, we employed analysis of variance (ANOVA) to analyze the data distribution across different seasons, assessing the variability in water quality indices. Furthermore, Pearson's correlation analysis Fig. 6 was utilized to examine the relationships between various water quality parameters. This approach allowed us to rigorously interpret the seasonal fluctuations and inter-parameter dependencies in water quality, critical for understanding the impacts and dynamics within the river system.

Multivariate statistical analyses were performed on the physical and chemical data utilizing OriginPro 2021 (Origin-Lab, Northampton, USA) to generate statistical summaries of the datasets (Awomuti et al. 2023). Piper trilinear diagram (Piper 1944) and Gibbs diagram (Gibbs 1970) were applied to determine surface water types, geochemical processes, geochemical influencing factors, and the categorization of surface water samples and their controlling mechanisms. Multivariate modeling techniques such as principal component analysis (PCA) are commonly utilized for assessing water quality. Therefore, by minimizing the chemical analysis data into common patterns, the correspondence analysis (CA) was used to identify the physicochemical characteristics based on their similarities (Kumar et al. 2020). The PCA was used to study the association between the physicochemical properties that were responsible for changes in water quality by converting the initial variables into a new set that reflected the effect of significant elements on water quality.

Results and discussion

DPSIR framework of river water quality and policy analysis

The DPSIR dynamic model was applied to determine factors that could influence the quality management of the Nyabarongo River (Wang et al. 2022a). The model utilizes driving forces (*D*), which define factors/interests that could lead to deterioration of the water quality status of the river; pressures that come about as a result of realizing the driving forces (*P*); states describe the spatio-temporal conditions of the river as a result of the exerted pressures (*S*); impacts (*I*) are the resulting short-long term effects on rivers species and responses are outcomes which can be formulated into policies to control pollution incidences of the river or reduce the effects (*R*). For the case of the Nyabarongo River, the DPSIR framework is shown in Fig. 7.

Drivers

Various factors have been identified in the literature as driving forces that lead to pressures on the quality of rivers. In the case of the Nyabarongo River, the main drivers identified during the study period were population growth, climate change, settlement, and urbanization around the river. Although the population of Rwanda is small comparable to other African countries, it was considered a key indicator contributing to the deterioration of the river quality. The population has risen gradually from 12,835,028 (2019) to 13,146,362 (2020), 13,461,888 (2021), and 13,776,698 (2022) (Squire and Nkurunziza 2021). With high population growth comes increased consumption and waste generation with improper disposal systems. The urbanization rate with many people resident in Kigali City (which was the closest city to the study area) is a direct correlation that could exert pressures on the river. As a result of urbanization, sewage and wastewater discharge into the Nyabarongo River can provide excess nitrogen and phosphorus, which lowers the water quality through eutrophication processes affecting aquatic life. The need for constant electricity has also seen the construction of hydroelectric dams along the river system which could potentially impact the river water quality (Kulimushi et al. 2021).

Pressure

Several tributaries connect to the Nyabarongo River implying that soil erosion from the basin of these rivers can impact the river of study increasing its suspended sediment composition (Kulimushi et al. 2021). Soil erosion is also formed due to agriculture resulting from the main driving force of the population growth rate, which exerts an influence on the quality and quantity of the river water (Bires and Raj 2020). Because agriculture is the most important sector of

the economy of Rwanda, chemical fertilizers used for this agricultural purpose contain phosphates and nitrates, which are known to be major contributors to water contamination. Eutrophication, which enriches the water surface with nutrients, is aided by nitrogen and phosphorus from the environment. The result of eutrophication is a proliferation of algae blooms (Shiferaw and Abebe 2021). Additionally, mismanagement of municipal solid and liquid waste (from domestic and industrial discharges) can result in disposal into the river which influences its quality over time (Omara et al. 2020).

States

The state of the Nyabarongo River is related to the values of river quality. These changes happen in the physical, chemical, and biological conditions of the river over time. In the context of the DPSIR framework, the changes observed in the water quality relate to the change in the existing natural physical, chemical, and biological properties of clean water as a result of one or more pressures. From the results of this study, there were several indications of the change in the quality of the river over the different climate seasons due to different identified pressures. Pressure derived from the driving forces has left the current condition of the river as having high dissolved solids, and high metal concentrations, resulting in some metals being major influences on the river water quality. High agricultural activities due to the increasing population and settlements around the river catchment will potentially result in increased eutrophication through the accumulation of fertilizers. Dead algal mats decaying in the water can cause terrible tastes and aromas, and their breakdown by bacteria depletes dissolved oxygen in the water, resulting in fish kills. Recent reports have also indicated a high risk in the African Lung Fish which is a dominant species of the river (Nteziyaremye and Omara 2020; Nteziyaremye et al. 2020; Omara et al. 2020).

Impact

The effects and impacts caused by the physical, chemical, and biological conditions of the river are directly correlated to human and ecological health risks. While the river provides enormous social and economic benefits, when contamination and pollution incidences increase, the water becomes hazardous to humans eventually depleting the capital goods it offers such as fish kills. Likewise, increased pollution in the river tends to cause a cost rise in the treatment of river water to meet desirable standards for consumption. The high pollution incidence of the river will impact household food consumption, especially access to fish produce. Additionally, with the agricultural system being largely dependent on the river, there is potential long-term bioaccumulation

of heavy metals through food webs which will impact the health status of the population at large (Umulisa et al. 2020).

Response

Several studies have indicated the important roles of stakeholders in providing adequate water services. Meanwhile, many countries are burdened with ensuring this service due to broader drivers and pressures. To resolve this, decision-making on water resource management needs to incorporate diverse knowledge in an accessible and meaningful manner (Kaur et al. 2020). This becomes necessary to support policy and its implementation to control factors that result in water quality degradation. In the case of the Nyabarongo River, the current operations of the WASAC can be expanded to include monitoring other rivers that join to exert similar regulatory controls and management practices to reduce water contamination and pollution (Moges et al. 2017). The government should put in restrictions and establishment of buffer zones around the river to avoid frequent agricultural and irrigation activity setups. New government policies on river water management and enforcement of industrial codes of practices are critical. This is necessary to reduce anthropogenic activities around the river (Malekmohammadi and Jahanishakib 2017). Agricultural conservation and land practices must be controlled through farmer-based education and proper spatial land planning. Regulation of operations within the catchment and watershed of the river system is important to reduce erosion of land-based activities into the river. Lastly, other institutions or ownerships should be included in the management of the river water quality by setting up a watershed management committee with clearly stated responsibilities. This will improve integration between various institutions and specify the owners who are responsible for maintaining the quality of the river.

Physical and chemical properties

The physicochemical characteristics of Nyabarongo River water have been investigated in some parts as helpful criteria for understanding the state of water geochemistry and related regulatory processes that play critical roles in the evolution of water quality (Karamage et al. 2016). Figure 2 and Table 7 show the behavior of water quality data across the seasons and statistical overview of datasets from the investigated surface water respectively. From Fig. 2, much of the dataset across the monitoring season within the years was distributed across the lower and upper percentile ranges presenting a general normal distribution. In the dry long season, the datasets were mostly left skewed except for datasets within June 2019 and August 2021 which were rightly skewed. In the dry short season, the datasets did not display any form of centrality. On average, the datasets from 2018
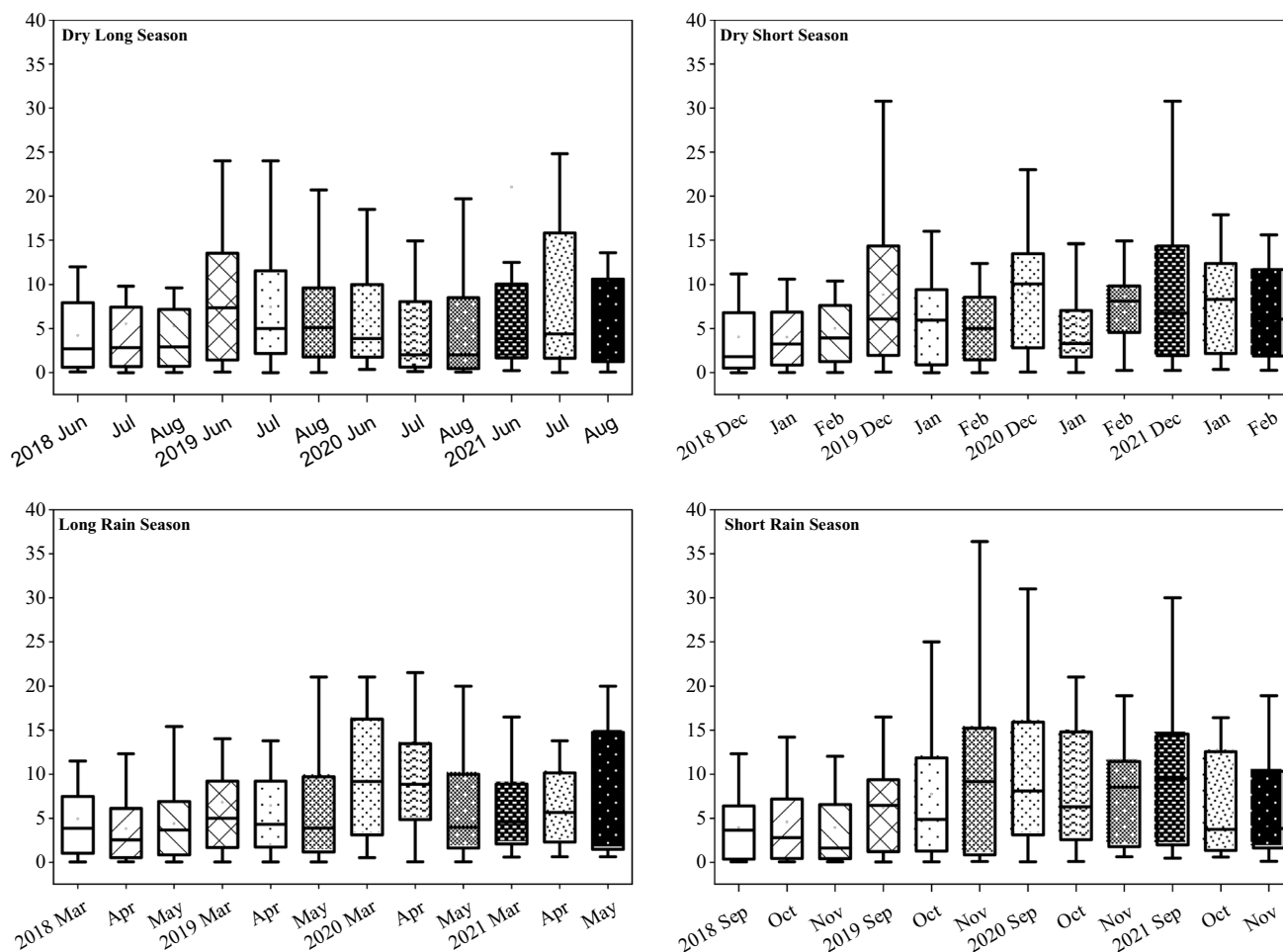
Fig. 2 The overall behavior and distribution of water quality data across the four seasons. The outcomes indicate the water quality in general is better during the long rainy season possibly due to the high precipitation effect and constant dissolution of water chemical constituents. The river hence becomes self-cleaning to reduce its contamination and pollution levels while the opposite could occur in the dry seasons

were left skewed as observed in the previous season, while the distribution was rightly skewed across most of the previous periods. The observations were similar to the long rain and short rain seasons.

Several water quality indicators, including pH, turbidity, and EC, is critical in expressing surface water quality. Therefore, these measures are the primary indicator metrics for assessing surface water quality and its degradation as a result of polluting activities. Water pH has a profound effect on the state such as metal dissolution, hardness, and alkalinity. The survival of most aquatic species is also impacted by pH as their metabolic activities are pH-dependent (Nteziyaremye and Omara 2020, Nteziyaremye et al. 2020). The obtained analytical datasets showed that pH had a mean of 8.7 ± 0.9 which indicated the water samples across the monitoring periods were virtually alkaline. The pH was slightly above WHO's standard limit of 8.5

for surface water bodies. Anthropogenic, climatic changes, and eutrophication could have significantly affected the water pH. The solubility of chemical constituents in particular metals is predominantly controlled by water pH, water temperature, and river flow. Lowered pH tends to increase competition between metal species and hydrogen ions for biding sites, while a decreased pH could cause the dissolution of metal carbonate complexes hence releasing free metal ions into the river column. (Kopáček et al. 2021).

Turbidity is a measure of the murkiness of water. The mean concentration (5.9 ± 1.6 NTU) was slightly above the WHO's limit standard of 5 NTU. The high murkiness of the river could be associated with regular erosion comprising silt, clay, organic matter, and plant debris into the river. Typically, transparency increases in correspondence to phases of seasonal succession (Sommer et al. 2012); in

Table 7 Descriptive statistics on water quality parameters

|	Mean	Standard deviation	Skewness	Kurtosis	CV	Min	Median	Max
pH	8.75	0.91	−0.93	−0.77	0.10	7.20	9.07	9.73
Turb (NTU)	5.91	1.62	−1.00	0.05	0.27	2.62	6.55	7.61
EC ($\mu S/cm^3$)	547.88	153.28	−0.57	−0.97	0.28	276.33	572.50	734.67
TDS (mg/L)	302.37	169.16	0.91	−0.30	0.56	137.60	218.45	678.33
HCO_3^- (mg/L)	123.36	13.82	−1.10	1.57	0.11	88.43	125.58	143.30
CO_3^{2-} (mg/L)	0.29	0.38	1.37	0.89	1.31	0.01	0.08	1.21
NO_3^- (mg/L)	12.03	5.13	1.74	5.18	0.43	3.60	11.52	27.33
PO_4^{3-} (mg/L)	7.41	5.22	0.72	−0.41	0.70	0.48	5.87	18.40
SO_4^{2-} (mg/L)	11.60	2.46	−0.20	−0.59	0.21	6.80	11.87	15.47
Cl^- (mg/L)	10.09	5.35	0.84	0.61	0.53	2.75	10.53	21.07
Ca^{2+} (mg/L)	9.04	2.73	−1.00	1.38	0.30	2.03	9.45	12.27
K^+ (mg/L)	14.05	28.46	3.04	9.30	2.03	0.48	4.82	109.47
Na^+ (mg/L)	5.30	5.85	0.76	−1.40	1.10	0.33	1.46	15.27
Mg^{2+} (mg/L)	15.28	9.20	2.05	5.27	0.60	7.60	14.41	43.30
Al^{3+} (mg/L)	9.14	9.31	1.18	1.71	1.02	0.22	9.79	33.53
Cu^{2+} (mg/L)	4.56	3.38	1.11	0.03	0.74	0.54	3.37	11.88
Fe^{3+} (mg/L)	7.86	5.72	0.94	−0.47	0.73	0.94	6.02	18.40
Mn^{2+} (mg/L)	3.84	4.63	1.48	1.36	1.20	0.20	1.37	15.57
Zn^{2+} (mg/L)	3.95	4.70	1.40	0.47	1.19	0.36	1.66	14.20
Br^- (mg/L)	7.09	8.78	2.06	3.62	1.24	0.70	3.42	31.67
CN^- (mg/L)	3.92	8.34	3.39	12.21	2.13	0.09	0.72	33.53
F^- (mg/L)	4.14	4.57	1.88	2.80	1.11	0.61	2.06	15.67
Cr^{3+} (mg/L)	3.76	3.90	2.58	7.93	1.04	0.20	2.64	16.49

this case, high transparency occurs in the long dry and short dry seasons. TDS and EC are directly related in revealing levels of dissolved solids and the corresponding electrical potential of the water. Therefore, high TDS directly infers high EC (Gad et al. 2020). From the datasets obtained across the monitoring seasons, the mean TDS value was (302.4 ± 169.2 mg/L) and EC was (547.9 ± 153.3 μS/cm³). These were below (WHO 2017) standard limits of 500 mg/L and 400 μS/cm³ which reflected a fresh water type. Nutrients were characterized by NO_3^-, SO_4^{2-}, and PO_4^{2-} with mean concentrations of 12 ± 5.1 mg/L, 11.6 ± 2.5 mg/L, and 7.4 ± 5.2 mg/L. The measured concentrations were below (WHO 2022) standard limits of 50 mg/L, 250 mg/L, and 50 mg/L, respectively. Ionic concentrations on average were above (WHO 2017) limit and increased in order $HCO_3^- > Mg^{2+} > K^+ > Cl^- > Ca^{2+} > Br^- > Na^+ > Cu^{2+} > F^- > Zn^{2+} > CN^- > Cr^{3+} > Fe^{3+} > Mn^{4+} > CO_3^{2-}$. The results revealed that HCO_3^- (123.4 ± 13.8) was the dominant anion and Mg^{2+} (15.3 ± 9.2) was the dominant cation which could influence water controlling processes.

Geochemical facies and controlling mechanisms

To better reveal an understanding of the geochemical mechanism influencing water quality and hydro chemical data of the Nyabarongo River, the water quality datasets were further analyzed by trilinear plots. Piper diagram shows the relative proportions of major ions in the water samples. The colors green, blue, and red typically represent different hydro-chemical facies, (green: calcium bicarbonate type, blue: sodium sulfate type, red: mixed type). Piper diagrams could reveal the prevalent cations and anions in the investigated water samples to define any geochemical facies. From Fig. 3, it is seen that in the dry long and short seasons, the water quality was most formed by calcium bicarbonate composition. In the long rain season, the water quality was formed by sodium sulfate composition, similar to the short rain season. The observations indicated that the geological weathering process could be highly influential in establishing the water chemistry of the Nyabarongo River. This was found in similar studies like that of Regina Irunde et al. (2022).

To further confirm this, the Gibbs diagram in Fig. 4 was used to understand the relationship between water chemical components relying on the association between TDS, $Na^+/(Na^+ + Ca^{2+})$, and $Cl^-/(Cl^- + HCO_3^-)$. The degree and quality of characteristics of the water are identified from three distinct fields, namely, precipitation dominance, evaporation dominance, and rock-water interaction dominance where all ions were expressed in in meq/l in this study. The surface water quality datasets were
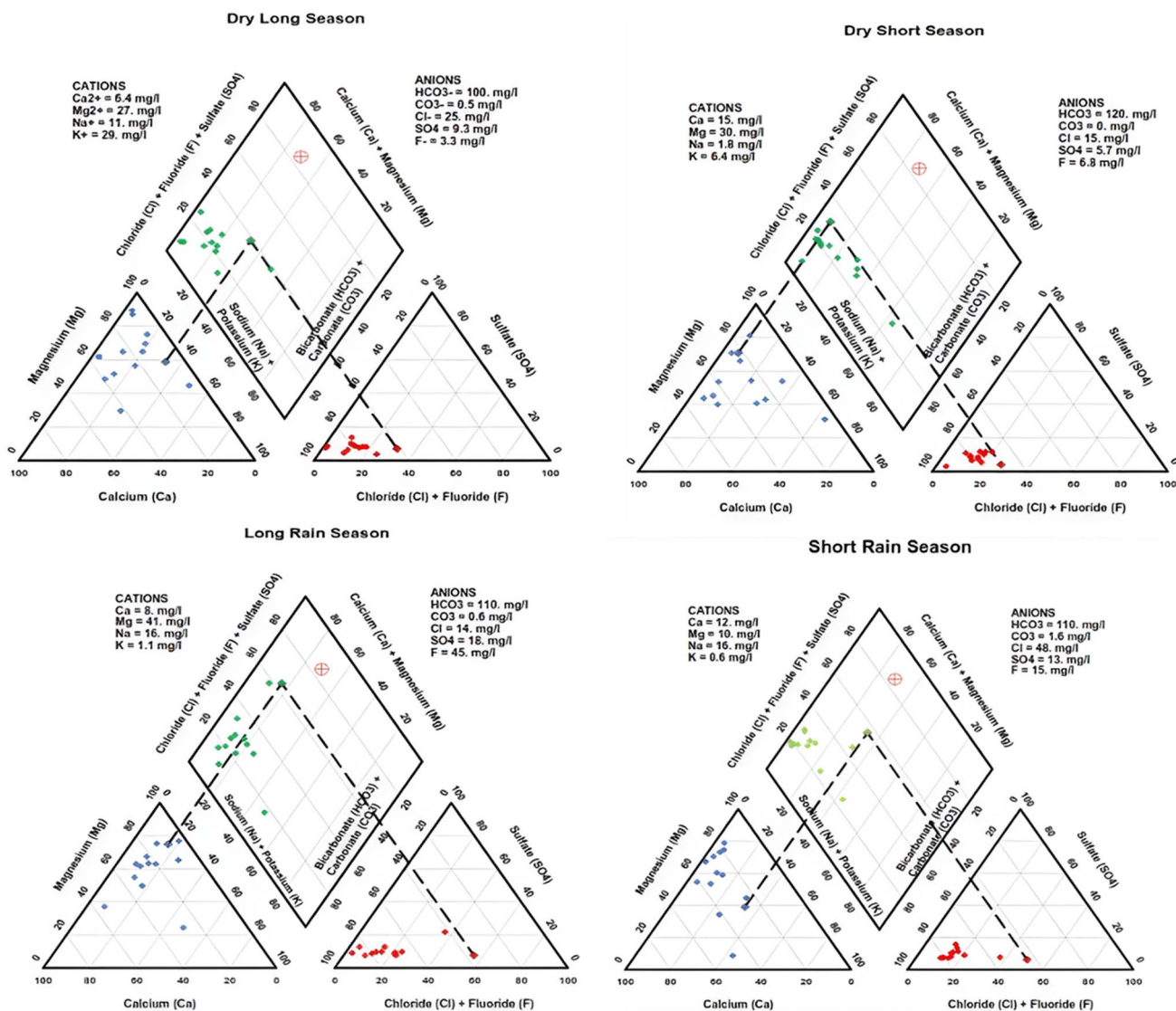
Fig. 3 Piper diagram showing the hydro-chemical facies of water samples from the Nyabarongo River across different seasons (green: calcium bicarbonate type, blue: sodium sulfate type, red: mixed type). The figure portrays that in the long and short dry seasons, the water quality was most formed by calcium bicarbonate composition. In the long rain season, the water quality was formed by sodium sulfate composition, similar to the short rain season. The observations indicated that the geological weathering process could be highly influential in establishing the water chemistry of the Nyabarongo River

distributed along the evaporation field which was influential in determining the factors controlling surface water quality. High evaporation rates as controlling mechanisms of the water formation could potentially contribute to high ionic concentrations investigated as similarly reported by (Giri and Singh 2014).

Water quality index

The WQI model was applied to assess surface water quality and measure the potability of the Nyabarongo River for drinking water purposes and values across the

monitoring seasons shown in Table 8. The maximum computed WQI from the water quality samples across the monitoring seasons was 52.90 (dry long), 21.478 (dry short), 93.66 (long rain), and 37.4 (short rain). Based on CCME 2001, the water quality across the monitoring seasons of the years could be described as marginal (WQI 45–65) for the dry long seasons, poor (WQI 0–44) for the dry short period, good (WQI: 80–94) for the long rains season, and poor (WQI 0–44) for the short rain season. The outcomes indicate the water quality in general is better during the long rainy season possibly due to the high precipitation effect and constant dissolution of water

Fig. 4 Gibbs plot of water quality formation and lithological characteristics. This was used to understand the relationship between water chemical components relying on the association between TDS, $Na^+/(Na^+ + Ca^{2+})$, and $Cl^-/(Cl^- + HCO_3^-)$. High evaporation rates as controlling mechanisms of the water formation could potentially contribute to high ionic concentrations
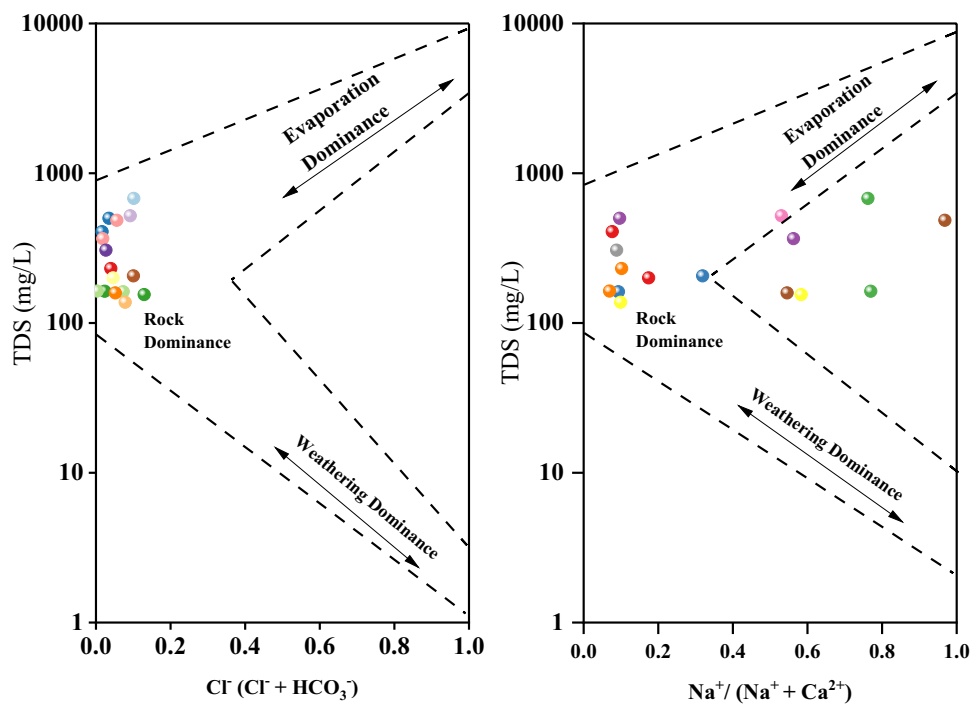
Table 8 Drinking water quality index across seasons (2018–2021)

| Parameter	Dry long	Dry short	Long rain	Short rain
pH	0.458	0.454	0.458	0.462
Turbidity (NTU)	0.642	0.973	1.006	0.958
EC ($\mu S/cm^3$)	0.001	0.001	0.001	0.001
TDS (mg/L)	0.004	0.004	0.005	0.005
HCO_3^- (mg/L)	0.036	0.031	0.030	0.033
CO_3^{2-} (mg/L)	0.000	0.000	0.000	0.000
NO_3^- (mg/L)	0.025	0.018	0.015	0.015
PO_4^{3-} (mg/L)	0.007	0.012	0.014	0.012
SO_4^{2-} (mg/L)	0.001	0.001	0.001	0.001
Cl^- (mg/L)	0.007	0.006	0.006	0.008
Ca^{2+} (mg/L)	0.180	0.270	0.213	0.288
K^+ (mg/L)	0.001	0.001	0.000	0.000
Na^+ (mg/L)	0.000	0.000	0.000	0.000
Mg^{2+} (mg/L)	0.027	0.021	0.023	0.022
Al^{3+} (mg/L)	2797.5	3100.2	4515.1	3420.9
Cu^{2+} (mg/L)	3.882	4.080	4.299	4.987
Fe^{3+} (mg/L)	202.6	242.8	395.1	480.1
Mn^{2+} (mg/L)	598.9	2642.0	819.7	1752.3
Zn^{2+} (mg/L)	1.635	1.118	0.872	3.011
Br^- (mg/L)	7.382	5.677	9.879	3.894
CN^- (mg/L)	2.558	8.351	34.829	13.511
F^- (mg/L)	0.654	0.569	1.408	1.281

chemical constituents (Das et al. 2022). The river hence becomes self-cleaning to reduce its contamination and pollution levels while the opposite could occur in the dry seasons.

Pollution and metal indices

Pollution indices (PIs) describe an efficient approach to characterize the quality of drinking water based on specified metal parameters (Kachroud et al. 2019). The metal indices (MI) of the water samples across the seasons varied from 0.2 to 433.0 for dry long, 0.1 to 174.3 for dry short, 0.1 to 223.7 for long rain, and 0.3 to 252.5 for short rain. According to the categorization of PI levels, the PI values indicated that the samples were not affected by K^+ and Cr^{3+}, (PI < 1.0) across all seasons but were strongly affected by Cu^{2+} (PI = 3–5) across all seasons and moderately affected by Al^{3+} (PI = 2–3), as presented in Table 9. However, the effects of Mn^{4+}, and Zn^{2+}, varied across the seasons, while Fe^{3+} (PI > 5) severely affected the water quality across the monitoring period as presented in Table 9. The high impact of Fe^{3+} could be associated with the lithogenic process of bedrock weathering over time (Xiao et al. 2015). Overall, it can be found that PI significantly influences the water quality across different climate seasons.

Table 9 Metal index and pollution index

ID	Parameters	Metal index	Pollution index	Class	Description
1	K^+(mg/L)	9.122223	1.513481	5	Seriously affected
2	Mg^{2+}(mg/L)	433	11.28051	5	Seriously affected
3	Al^{3+}(mg/L)	16.76667	2.054183	3	Moderately affected
4	Cu^{2+}(mg/L)	39.6111	3.218004	5	Seriously affected
5	Fe^{3+}(mg/L)	184	6.953416	5	Seriously affected
6	Mn^{2+}(mg/L)	5.18889	1.146262	3	Moderately affected
7	Zn^{2+}(mg/L)	7.1	1.349228	2	Slightly affected
8	Cr^{3+}(mg/L)	0.329867	0.288892	1	No effect
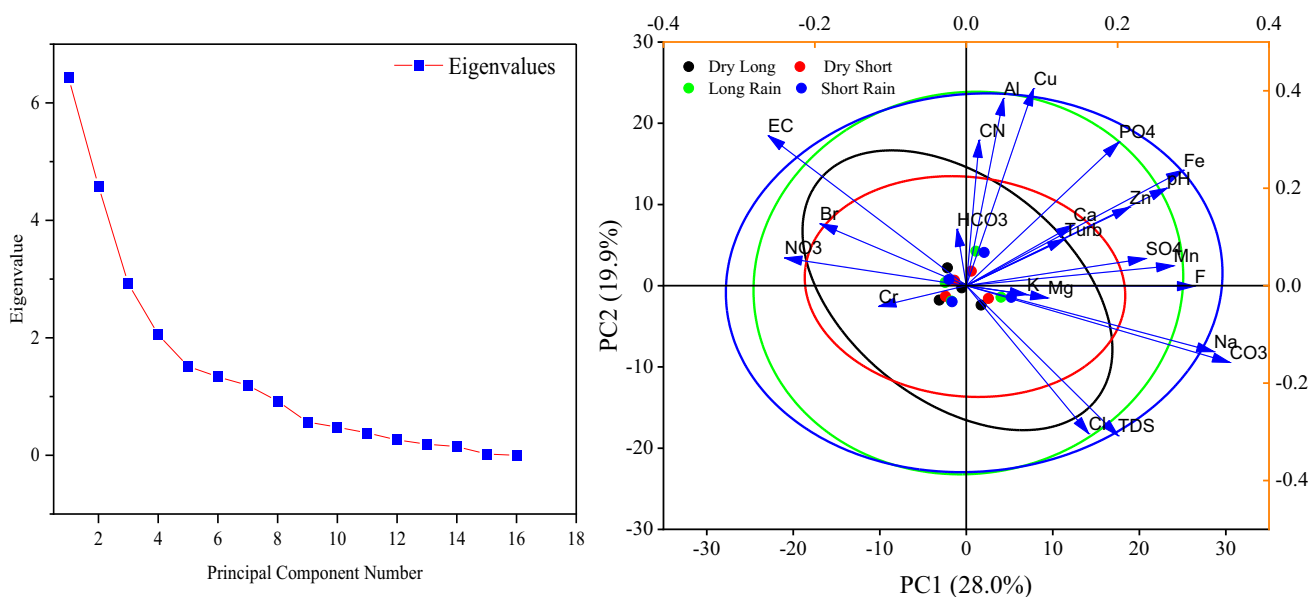
Fig. 5 Screen plot of eigenvalues (left) and PCA biplot (right) of water samples. It displays the principal component analysis findings for the physicochemical properties obtained from the surface water samples

Principal component analysis

PCA findings for the physicochemical properties obtained from the surface water samples are shown in Fig. 5. The first principal component (PC1) explained 24.6% of the variation in the datasets, while the second principal component (PC2) explained 23.2% of total variation. Along PC1, Cl^-, TDS, SO_4^{2-}, PO_4^{3--}, Mg^{2+}, K^+, and Na^+ could reveal their concentrations were contributed by similar sources (Samtio et al 2022). Cr^{3+}, Br^-, and NO_3^-, on the other hand, were inversely related which could be contributed by anthropogenic sources. NO_3^- for instance could be contributed by fertilizer runoff from farming activities along the river and other household depositions of greywater. Metals including

Mn^{4+}, Cu^{2+}, CN^-, and Fe^{3+} could explain their sources were possibly generated from the rivers' baseline conditions (Wang et al. 2017).

Pearson correlation analysis

Pearson correlation analysis was performed to further reveal the relationship between measured physicochemical properties shown in Fig. 6. In the dry long season, significant negative associations were observed between pH and NO_3^- ($r = -0.97$, $p = 0.026$) as well as between pH and Fe^{3+} ($r = -0.99$, $p = 0.0049$). Ca^{2+} and HCO_3^- also displayed a strong negative correlation ($r = -0.95$, $p = 0.644$) as well between Na^+ and HCO_3^- ($r = 0.99$, $p = 0.00033$).
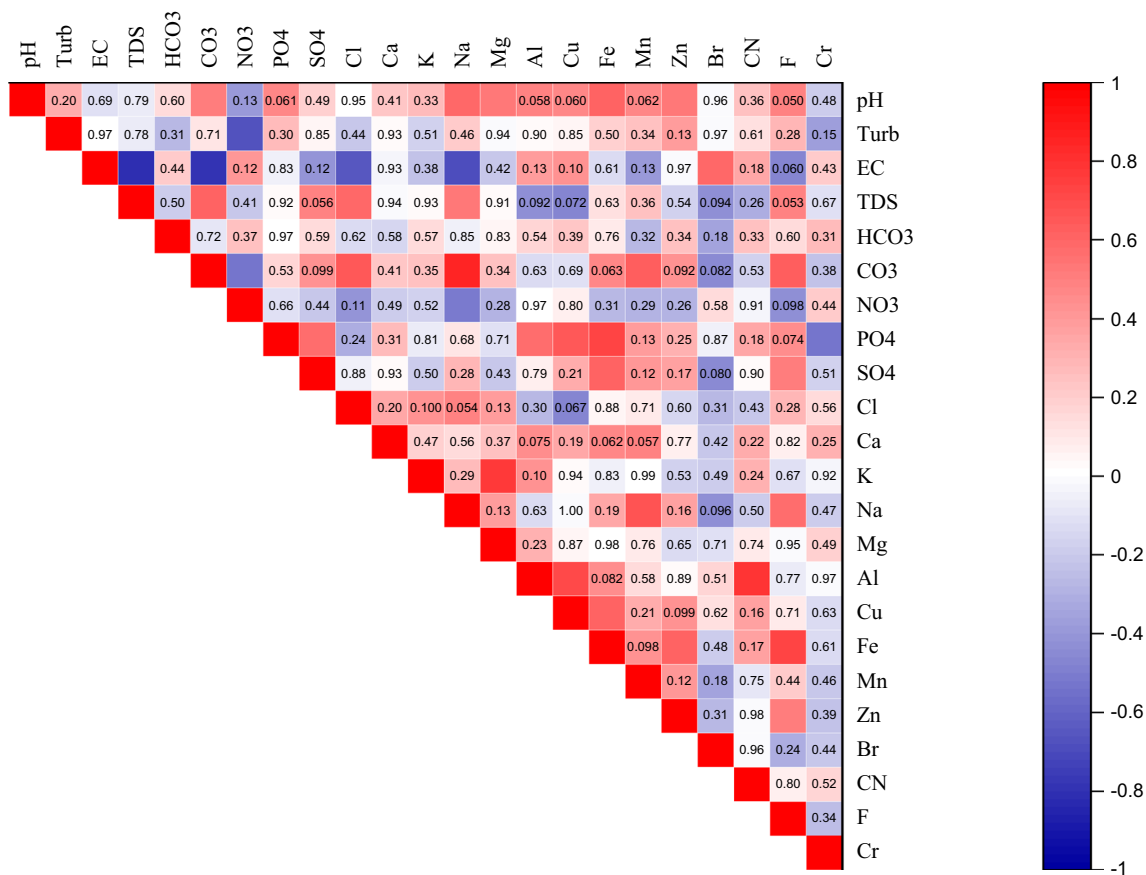
Fig. 6 Pearson correlation analysis plot was performed to further reveal the relationship between measured physicochemical properties

The negative correlation between various parameters could originate from different factors including biological processes, such as photosynthesis and microbial activities. Geological factors like calcium carbonate-rich formations and anthropogenic influences such as agricultural runoff further affect the water quality. Additionally weathering processes of rocks and minerals in the river catchment area release ions into the water which makes strong connection with the Rwanda Water Board Annual Report 2021 (Portal 2021). On other hand, Fe^{3+} correlated positively with NO_3^- at $r = 0.97$, $p = 0.024$, while a similar strong correlation between Cu^{2+} and PO_4^{3-} were determined at $r = 0.97$, $p = 0.024$. Fe^{3+}, Cu^{2+}, NO_3^-, and PO_4^{3-} are typical constituents of fertilizer and pesticides and hence could be a major reason for their association (Stackpoole et al. 2019). Similar strong positive correlations between Br^- and CN^- with PO_4^{2-} were at $r = 0.99$, $p = 0.053$ and $r = 0.98$, $p = 0.016$, respectively. Amongst the cations, Mg^{2+} displayed strong association with K^+ ($r = 0.98$, $p = 0.014$). In the dry short season, a similar trend of strong positive and negative associations was established between the various ionic components. The association between EC and TDS was displayed with a strong negative correlation at

$r = -0.97$, $p = 0.023$. While HCO_3^- also correlated with EC at $r = 0.95$, $p = 0.045$ and HCO_3^- with TDS at $r = 0.96$, $p = 0.035$. Mg^{2+} displayed a strong correlation with pH at $R^2 = 0.95$, $p = 0.046$, while Mn also showed a similarly strong positive correlation with Na^+ ($r = 0.98$, $p = 0.010$). Zn^{2+} correlated positively with Al^{3+} ($r = 0.99$, $p = 0.038$) and Cu^{2+} ($r = 0.98$, $p = 0.041$). In the long rainy season, a similar trend of strong positive associations within the cations was determined. Al^{3+} correlated positively with Ca^{2+} ($r = 0.99$, $p = 0.00078$) and K^+ ($r = 0.99$, $p = 0.00064$). Similar observations were made with Cu^{2+} and Ca^{2+}, K^+ at $r = 0.95$, $p = 0.04$ and $r = 0.96$, $p = 0.034$, respectively. Likewise, Fe^{3+} and Mn^{4+} correlated strongly with Ca^{2+} and K^+ at $r = 0.99$), respectively. Strong negative associations were on the other hand established between Cl^- and EC ($R^2 = -0.97$, $p = 0.026$) and NO_3^- ($r = -0.99$, $p = 0.0066$). In the short rainy season, there was a very less strong correlation with the different chemical constituents. Similarly, pH positively correlated with Ca^{2+} ($r = 0.95$, $p = 0.04$), while Na^+ showed a positive correlation with NO_3^- ($r = 0.99$, $p = 0.069$). CN^- and Cr^- were strongly correlated negatively with turbidity ($r = 0.96$, $p = 0.039$) and ($r = 0.98$, $p = 0.012$), respectively. Both Na^+ and

Table 10 Non-carcinogenic risk hazard index (HI) of heavy metals in river

HM	Ingestion		Dermal	
	Adult	Child	Adult	Child
Cu^{2+}	7.68E−07	5.02E−06	5.77E−09	2.89E−08
Mn^{2+}	3.52E−08	2.30E−07	1.32E−09	6.61E−09
Zn^{2+}	8.89E−08	5.81E−07	6.68E−10	3.34E−09
Cr^{3+}	8.44E−06	5.51E−05	5.07E−07	2.54E−06

HM-Heavy metal

Table 11 Carcinogenic risk of heavy metal (Cr) in river

HM	Ingestion		Dermal	
	Adult	Child	Adult	Child
Cr^{3+}	4.22E−06	6.89E−06	2.53E−07	3.17E−07

F^- correlated positively with HCO_3^- at $r = 0.99$, $p = 0.006$ and $r = 0.98$, $p = 0.011$. The strong high correlation within the chemical constituents could infer they were typically originating from identical sources across the varying seasons. Nonetheless, some more information on the source and pathways of heavy metals could be relevant to provide the correlation between the inter-elements (Zhang et al. 2018).

Non-carcinogenic and carcinogenic human health risk assessment

Non-carcinogenic and carcinogenic risk of heavy metals through oral ingestion (M_{ing}) and dermal contact (M_{dermal}) to adults and children were estimated and results are presented in Tables 10 and 11, respectively. It is observed that the hazard index (HI) of four heavy metals, Cu, Mn, Zn,
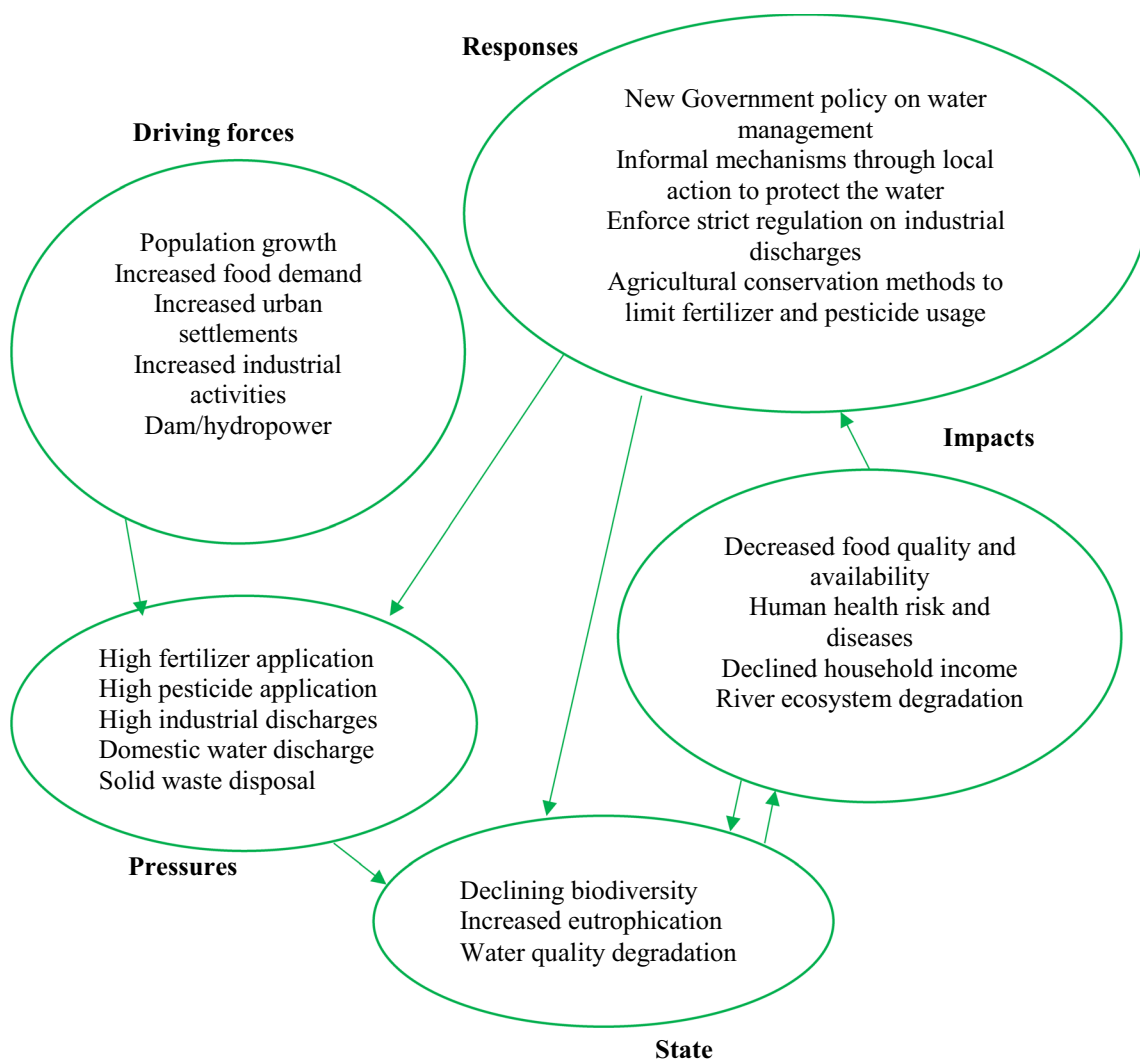
Fig. 7 DPSIR framework of Nyabarongo River that determines factors that could influence the quality and the management of the Nyabarongo River

and Cr, were below the standards, i.e., HI < 1, and ranged from $8.89E-08$ to $7.68E-07$ for oral ingestion in adults, and $2.30E-07$ to $5.02E-06$ for oral ingestion in children. For dermal contact, the HI in adults ranged from $6.68E-10$ to $5.07E-07$, while in children $6.61E-09$ to $2.54E-06$. Due to the lack of estimated slope factors of other heavy metals, the carcinogenic risk of Cr^{2+} was estimated. The results indicated a total carcinogenic risk (TCR) of less than 1 for both oral ingestion and dermal contact (TCR $< 10^{-6}$ and TCR $< 10^{-7}$) indicating no health risk. Nonetheless, it is important that the concentration of heavy metals be constantly monitored and enhance the water treatment system.

Conclusion

In this study, a DPSIR model was developed to identify primary factors contributing to water quality decline, evaluate their seasonal impacts, and craft specific responses (Fig. 7). The results from this study applied statistical approaches to evaluate the water quality of the Nyabarongo River and established a drinking water quality index. The acceptability of the water quality differed across the four main climatic seasons existing in Rwanda, ranging from poor to good, and marginal according to the Canadian Council of Ministers of Environment (Saffran et al. 2001). The water chemistry was found to mainly be formed out of evaporation of lithological constituents. Multivariate analysis could reveal that the water quality is influenced by both anthropogenic (agricultural, industrial discharges, household discharges, poor sanitation) and possible long-term natural causes (lithological weathering of the river bedrock). Ion concentrations surpassed the guidelines set by the World Health Organization (WHO), with prevalent ions identified as bicarbonate (HCO_3^-) and magnesium (Mg^{2+}). The fluctuations in water quality across seasons were driven by factors such as increased prevalence of calcium bicarbonate during dry periods and elevated presence of sodium sulfate during rainy periods. Pollution indices were associated with Fe^{3+} and Mg^{2+} concentrations. Health risk assessment for both adults and children revealed that heavy metals in rivers may not pose significant threats, yet send strong signals to governmental management since the Nyabarongo River is a major source of drinking water in the country. The results obtained are significant inputs towards developing drinking water quality guidelines in Rwanda and contributing towards meeting SDG 6.

Declarations

References

American Public Health Association A (1999) Standard method for examination of water and wastewater. American public health association, american water works association, water environment federation. https://dl.icdst.org/pdfs/files/9b8d1f12b54f315 4c8c648e0ec810185.pdf

Awomuti A et al (2023) Towards adequate policy enhancement: an AI-driven decision tree model for efficient recognition and classification of EPA status via multi-emission parameters. City and Environment Interactions 20:100127

Basin (2022) Drinking water and water resources. Interstate commission on the potomac river basin. https://www.potomacriver.org/about-icprb/

Benjamin G (2015) Assessment of micro to small hydropower potential sites of Nyabarongo river basin of Rwanda. Ethiopia, Arba Minch University, MSc

Bires Z, Raj S, (2020) Tourism as a pathway to livelihood diversification: evidence from biosphere reserves, Ethiopia. Tour Manag 81:104159. https://doi.org/10.1016/j.tourman.2020.104159

Brown RM et al (1972) A water quality index — crashing the psychological barrier. Indicators of Environmental Quality, Boston, MA, Springer, US

Caeiro S et al (2005) Assessing heavy metal contamination in Sado Estuary sediment: an index analysis approach. Ecol Ind 5(2):151–169

Camara J, Abdullah AFB et al (2019) Spatiotemporal assessment of water quality monitoring network in a tropical river. Environ Monit Assess 191:729

Chen K, Gao Shen (2022) Assessment of urban river water pollution with urbanization in East Africa. Environ Sci Pollut R 29:40812–40825

Chen Y, Yu P, Wang L, Chen Y, Chan EHW (2024). The impact of rice-crayfish field on socio-ecological system in traditional farming areas: implications for sustainable agricultural landscape transformation. J Clean Prod 434:139625. https://doi.org/10.1016/j.jclepro.2023.139625

Das M, Semy K, Kuotsu K (2022) Seasonal monitoring of algal diversity and spatiotemporal variation in water properties of Simsang river at South Garo Hills, Meghalaya, India. Sustain Water Resour Manag 8:16. https://doi.org/10.1007/s40899-022-00611-6

European Environment Agency (2017) Surface water quality monitoring - summary. The UK and internationalmonitoring programmes. European Environment Agency. https://www.eea.europa.eu/publications/92-9167-001-4/page008.html

European Environment Agency (2020) Surface water quality monitoring summary—France. from https://www.eea.europa.eu/publications/92-9167-001-4/page008.html. Accessed Dec 2023

Gad M et al (2020) Combining water quality indices and multivariate modeling to assess surface water quality in the Northern Nile Delta. Egypt. Water 12(8):2142

Gibbs RJ (1970) Mechanisms controlling world water chemistry. Science 170(3962):1088–1090

Giri S, Singh AK (2014) Assessment of surface water quality using heavy metal pollution index in Subarnarekha River. India Water Qual Expo Health 5(4):173–182

Goher ME et al (2019) Water quality status and pollution indices of Wadi El-Rayan lakes, El-Fayoum. Egypt Sustain Water Resour Manag 5(2):387–400

Halisçelik E, Soytas MA (2019) Sustainable development, vol 27, no. 4. Wiley Online Library. https://doi.org/10.1002/sd.1869

Holzforster F, Schmidt U (2007) Anatomy of a river drainage reversal in the Neogene Kivu-Nile Rift. Quat Sci Rev 26(13–14):1771–1789

Irunde R, Ijumulana J, Ligate F, Maity JP, Ahmad A, Mtamba JOD, Mtalo F, Bhattacharya P (2022) Arsenic in Africa: potential sources, spatial variability, and the state of the art for arsenic removal using locally available materials. Groundwater Sustain Dev 18. https://api.semanticscholar.org/CorpusID:247486565

Kachroud M, Trolard F, Kefi M, Jebari S, Bourri G (2019) Water quality indices: challenges and application limits in the literature. Water 11(2). https://api.semanticscholar.org/CorpusID:133798554

Karamage F et al (2016) USLE-based assessment of soil erosion by water in the Nyabarongo river catchment. Rwanda Int J Environ Health Res 13(8):835

Kaur M et al (2020) Investigating the impacts of urban densification on buried water infrastructure through DPSIR framework. J Clean Prod 259:120897

Kayembe JM, Sivalingam P, Salgado CD, Maliani J, Ngelinkoto P, Otamonga J-P, Mulaji CK, Mubedi JI, Poté J (2018) Assessment of water quality and time accumulation of heavy metals in the sediments of tropical urban rivers: case of Bumbu River and Kokolo Canal, Kinshasa City, Democratic Republic of the Congo. J Afr Earth Sci 147:536–543. https://doi.org/10.1016/j.jafrearsci.2018.07.016

Kopáček J et al (2021) Biogeochemical causes of sixty-year trends and seasonal variations of river water properties in a large European basin. Biogeochemistry 154(1):81–98

Kulimushi L et al (2021) Erosion risk assessment through prioritization of sub-watersheds in Nyabarongo river catchment. Rwanda Environ Challenges 5:100260

Kumar V et al (2020) Assessment of heavy-metal pollution in three different Indian water bodies by combination of multivariate analysis and water pollution indices. Um Ecol Risk Assess 26(1):1–16

Kumar B, Singh UK, Ojha SN (2018) Evaluation of geochemical data of Yamuna River using WQI and multivariate statistical analyses: a case study. Int J River Basin Manag 17(2):143–155. https://doi.org/10.1080/15715124.2018.1437743

Kwisanga JMP (2017) Assessing flood risk and developing a framework for a mitigation strategy under current and future climate scenarios in Nyabarongo Upper Catchment, Rwanda. https://repository.pauwes-cop.net

Li W, Qi J, Huang S, Fu W, Zhong L, He B-J (2021) A pressure-state-response framework for the sustainability analysis of water national parks in China. Ecol Indic 131:108127. https://doi.org/10.1016/j.ecolind.2021.108127

Malekmohammadi B, Jahanishakib F (2017) Vulnerability assessment of wetland landscape ecosystem services using

driver-pressure-state-impact-response (DPSIR) model. Ecol Ind 82:293–303

Moges M et al (2017) Water quality assessment by measuring and using Landsat 7 ETM+ images for the current and previous trend perspective: Lake Tana Ethiopia. J Water Resource Prot 9:1564–1585

Mohseni U et al (2022) An innovative approach for groundwater quality assessment with the integration of various water quality indexes with GIS and multivariate statistical analysis—a case of Ujjain City. Waer. Cons. Sci & Eng, India

He N, Zhou Y, Li W, Li Q, Zuo Q, Liu J, Li M (2022) Spatiotemporal evaluation and analysis of cultivated land ecological security based on the DPSIR model in Enshi autonomous prefecture, China, vol. 145. Elsevier, United Kingdom. https://www.sciencedirect.com/journal/ecologica

Nteziyaremye P, Omara T (2020) Bioaccumulation of priority trace metals in edible muscles of West African lungfish (Protopterus annectens Owen, 1839) from Nyabarongo River. Rwanda Cogent Environ Sci 6(1):1779557

Nteziyaremye P, Omara T, Li F (2020) Bioaccumulation of priority trace metals in edible muscles of West African lungfish (Protopterus annectens Owen, 1839) from Nyabarongo River, Rwanda. Cogent Environ Sci 6(1). https://doi.org/10.1080/23311843.2020.1779557

Ojekunle O et al (2016) Evaluation of surface water quality indices and ecological risk assessment for heavy metals in scrap yard neighbourhood. Springerplus 5:560

Omara T, Nteziyaremye P, Akaganyira S et al (2020) Physicochemical quality of water and health risks associated with consumption of African lung fish (Protopterus annectens) from Nyabarongo and Nyabugogo rivers, Rwanda. BMC Res Notes 13:66. https://doi.org/10.1186/s13104-020-4939-z

Piper AM (1944) A graphic procedure in the geochemical interpretation of water-analyses. EOS-Trans Am Geophys Union 25(6):914–928

Portal RW (2021) Surface water monitoring report. from https://waterportal.rwb.rw. Accessed Feb 2024

Qin X, Hu X, Xia W (2003) Investigating the dynamic decoupling relationship between regional social economy and lake water environment: the application of DPSIR-Extended Tapio decoupling model. J Environ Manag 345:118926. https://doi.org/10.1016/j.jenvman.2023.118926. Accessed 1 Nov 2023

Saffran KS, Cash KJ, Hallard KA, Wright R (2001) Canadian water quality guidelines for the protection of aquatic life CCME water quality index 1.0 User's Manual. https://api.semanticscholar.org/CorpusID:2789561

Samtio R, Rajper KH, Hakro AAaD et al (2022) Impact of water–sediment interaction on hydrogeochemical signature of dug well aquifer by using geospatial and multivariate statistical techniques of Islamkot sub-district, Tharparkar district, Sindh, Pakistan. Arab J Geosci 15:167. https://doi.org/10.1007/s12517-022-09436-1

Shiferaw M, Abebe R (2021) A spatial analysis and modeling study of sedimentation impacts on dams found in south Gondar zone Ethiopia. Modeling Earth Syst Environ 7(4):2225–2230

Sommer U et al (2012) Beyond the plankton ecology group (PEG) model: mechanisms driving plankton succession. Annu Rev Ecol Evol Syst 43(1):429–448

Squire JNT, Nkurunziza J (2021) Urban waste management in post-genocide Rwanda: an empirical survey of the City of Kigali. J Asian Afr Stud 57(4):760–772

Stackpoole SM et al (2019) Variable impacts of contemporary versus legacy agricultural phosphorus on US river water quality. Proc Natl Acad Sci 116(41):20562–20567

Tamasi G, Cini R (2004) Heavy metals in drinking waters from Mount Amiata (Tuscany, Italy). Possible risks from arsenic for public health in the Province of Siena. Sci Total Environ 327(1):41–51

Umulisa V et al (2020) First evaluation of DDT (dichlorodiphenyltrichloroethane) residues and other Persistence Organic Pollutants

in soils of Rwanda: Nyabarongo urban versus rural wetlands. Eco-toxicol Environ Saf 197:110574

Wang J et al (2017) Multivariate statistical evaluation of dissolved trace elements and a water quality assessment in the middle reaches of Huaihe River, Anhui, China. Sci Total Environ 583:421–431

Wang B et al (2022a) A SEEC model based on the DPSIR framework approach for watershed ecological security risk assessment: a case study in Northwest China. Water 12:1534

Wang B, Yu F, Teng Y, Cao G, Zhao D, Zhao M (2022b) A SEEC model based on the DPSIR framework approach for watershed ecological security risk assessment: a case study in Northwest China. Water 14:106. https://doi.org/10.3390/w14010106

WHO (2017) Guidelines for drinking-water quality: 4th edition, incorporating the 1st addendum. World Health Organization. https://www.who.int/publications/i/item/9789241549950. Accessed 24 Apr 2017

Xiao Y-H et al (2015) Iron as a source of color in river waters. Sci Total Environ 536:914–923

Yan Zhou LZ (2016) Impact analysis of the implementation of cleaner production for achieving the low-carbon transition for SMEs in the Inner Mongolian coal industry. Cleaner Production 127:418–424

Zhang Z et al (2018) Assessment of heavy metal contamination, distribution and source identification in the sediments from the Zijiang River, China. Sci Total Environ 645:235–243

Zhang R et al (2020) Health risk assessment of heavy metals in agricultural soils and identification of main influencing factors in a typical industrial park in northwest China. Chemosphere 252:126591

Authors and Affiliations

Mycline Umuhoza[1] · Dongjie Niu[1,2,3] · Fengting Li[1,2,3]

✉ Dongjie Niu
niudongjie@tongji.edu.cn

[1] College of Environmental Science and Engineering, Tongji University, 1239 Siping Rd., Shanghai 200092, China

[2] State Key Laboratory of Pollution Control and Resource Reuse, College of Environmental Science and Engineering, Tongji University, 1239 Siping Rd., Shanghai 200092, China

[3] Shanghai Institute of Pollution Control and Ecological Security, North Zhongshan Rd. 1515, Shanghai 200092, China